18. M. Rexach, G. Blobel, *Cell* **83**, 683 (1995).
19. D. Görlich, P. Henklein, R. A. Laskey, E. Hartmann, *EMBO J.* **15**, 1810 (1996).
20. K. Weis, C. Dingwall, A. I. Lamond, *EMBO J.* **15**, 7120 (1996).
21. B. Kobe, *Nature Struct. Biol.* **6**, 388 (1999).
22. G. Cingolani, C. Petosa, K. Weis, C. W. Müller, *Nature* **399**, 221 (1999).
23. Emission spectra were analyzed with a Fluorolog 2 spectrophotometer controlled by Datamax 2.2 (Jobin Yvon Spex) and the Grams 3.04 II software package (Galactic Industries, Salem, NH). Both excitation and emission slits were set at 2 nm and voltage at 950 V.
24. Recombinant S-tagged Ran (2 μM) preloaded with either GTP or GDP was incubated with 4 μM purified YRC in phosphate-buffered saline on ice for 30 min. The Ran-GTP reaction was split into two aliquots, and one sample was treated with 100 ng of recombinant Ran-GAP. S-tagged importin β (2 μM) was incubated with recombinant importin α or YIC (each at 2 μM final concentration) in either the presence or absence of Ran preloaded with GTP (4 μM). Proteins bound to Ran or importin β were retrieved on protein-S-agarose beads, eluted with sample buffer, and analyzed by SDS–polyacrylamide gel electrophoresis (SDS-PAGE).
25. Dissociation constants between the YIC sensor, IBB, or importin α and β were measured with the Ran-GAP protection assay (*34*) (P. Kalab, K. Weis, R. Heald, unpublished data).
26. B. Catimel *et al.*, *J. Biol. Chem.* **276**, 34189 (2001).
27. Cytostatic factor (CSF)–arrested extracts of *Xenopus* eggs were supplemented with 500 demembranated *Xenopus* sperm nuclei/μl and X-rhodamine–labeled tubulin (0.1 mg/ml) to visualize microtubules. Entry into interphase was induced by the addition of 0.4 mM $CaCl_2$. If not indicated otherwise, 2 μM YRC or YIC probe was added. Both excitation and emission slits were set at 15 nm and voltage at 550 V.
28. A. W. Murray, *Methods Cell Biol.* **36**, 581 (1991).
29. Supplementary material is available on *Science* Online at www.sciencemag.org/cgi/content/full/295/5594/2452/DC1.
30. For pull-downs from extract with streptavidin beads, YIC and YRC were biotinylated with dithiothreitol (DTT)–cleavable biotinylation reagent (EZ-Link Sulfo-NHS-ss-Biotin, Pierce, no. 21331) according to the manufacturer's instructions in a 5:1 molar biotin excess, and dialyzed against XBG. Biotinylation did not inhibit probe FRET or affect in vitro binding interactions (P. Kalab, K. Weis, R. Heald, data not shown). Streptavidin beads (Pierce, no. 53117) were combined with biotinylated probes on ice for 20 min, washed with extract buffer (XB) (*28*), and mixed with 50 μl of CSF extract supplemented with either 30 μM Ran-Q69L-GTP or an equal volume of XB. After incubation at room temperature for 20 min, beads were pelleted and washed extensively, and bound proteins were eluted with 100 mM DTT and analyzed by SDS-PAGE and immunoblot with antibodies specific for Ran and importin β.
31. Images were collected with a ×40 Plan Fluor lens (Nikon) and a ×10 CFI objective using a Nikon E600 fluorescent microscope equipped with a cooled Hamamatsu charge-coupled device camera (C4742-98), Lambda 10-2 (Sutter) shutter controller, and a manual sliding filter cube holder (Nikon). The filter set for YFP emission fluorescence (I_{YFP}) consisted of exciter HQ500/20, dichroic Q515LP, and emitter HQ535/30. The CFP fluorescence (I_{CFP}) was collected with exciter D436/20, dichroic 455DCLP, and emitter D480/40. The CFP/YFP energy transfer emission (I_{FRET}) was imaged with exciter D436/20, dichroic 455DCLP, and emitter D535/30. X-rhodamine–labeled tubulin was visualized with an HQ-TRITC filter cube. All filters sets were made by Chroma. Images were acquired consecutively by TRITC (0.2 to 0.5 s) followed by YFP, CFP, and FRET cubes (with an identical setting within each sample, 1 or 2 s each) using Metamorph 4.6 imaging software (Universal Imaging) with no binning. I_{FRET}/I_{CFP} ratio images were calculated from 14-bit I_{FRET} and I_{CFP} images by Metamorph "Ratio" function and displayed in pseudocolor within the ratio range 0.7 to 1.3 for YRC samples and in the range 0.7 to 1.8 for YIC-containing samples. Images in 14 bits were converted to 8 bits with NIH Image 1.6, and all images were composed with Adobe Photoshop 5.5.
32. Z. Xia, Y. Liu, *Biophys. J.* **81**, 2395 (2001).
33. G. W. Gordon, G. Berry, X. H. Liang, B. Levine, B. Herman, *Biophys. J.* **74**, 2702 (1998).
34. We thank A. Dernburg and members of the Heald and Weis labs for helpful discussions and/or comments on the manuscript, M. Welch for help with fluorimetry, Y. Azuma for help with RCC1 purification, M. Ignatius for help with microscopy, and G. O. Nads for sperm nuclei. Funded by grants from NIH and the Pew Scholars Program (R.H.) and the Searle Scholars Program (K.W.).

7 December 2001; accepted 25 February 2002

Systemic RNAi in *C. elegans* Requires the Putative Transmembrane Protein SID-1

William M. Winston, Christina Molodowitch, Craig P. Hunter*

Double-stranded RNA-mediated gene interference (RNAi) in *Caenorhabditis elegans* systemically inhibits gene expression throughout the organism. To investigate how gene-specific silencing information is transmitted between cells, we constructed a strain that permits visualization of systemic RNAi. We used this strain to identify systemic RNA interference–deficient (*sid*) loci required to spread gene-silencing information between tissues but not to initiate or maintain an RNAi response. One of these loci, *sid-1*, encodes a conserved protein with predicted transmembrane domains. SID-1 is expressed in cells sensitive to RNAi, is localized to the cell periphery, and is required cell-autonomously for systemic RNAi.

One of the first reported and still mysterious aspects of RNAi in *C. elegans* is that it is systemic. Injection of gene-specific double-stranded RNA (dsRNA) into one tissue leads to the posttranscriptional silencing of that gene in other tissues and in that worm's progeny (*1*). The systemic nature of RNAi also provides for initiation of RNAi by soaking animals in dsRNA (*2*, *3*) or by cultivating worms on bacteria expressing dsRNA (*4*, *5*). Although systemic RNAi has not been demonstrated in any other animal, systemic post-transcriptional gene silencing (PTGS) effects in plants are well established (*6*, *7*). PTGS appears to play a role in viral defense (*8*); at the same time, viruses are able to inhibit systemic PTGS (*9*).

Genes required for RNAi have been identified in a variety of systems, as have small interfering RNAs (siRNAs) that can directly trigger RNAi and act as guide RNAs that direct sequence-specific mRNA cleavage (*10*–*12*). Among the *C. elegans* genes required for RNAi are *rde-1* and *rde-4*, which have no readily detectable mutant phenotype other than resistance to RNAi (*13*). These mutants are resistant to dsRNA targeting both somatic and germ line–specific genes and are also resistant to dsRNA produced by transgenes (*13*). However, these genes are not involved in systemic RNAi, because homozygous *rde-1* or *rde-4* mutant animals injected in the intestine with dsRNA are capable of efficiently transporting the RNAi effect to heterozygous cross progeny (*13*). It is noteworthy that *rde-4* is required for the efficient production of siRNAs (*14*), suggesting that siRNAs are not required for systemic RNAi.

To specifically investigate systemic RNAi, we constructed a transgenic strain (HC57) that allows simultaneous monitoring of localized and systemic RNAi. HC57 expresses two green fluorescent protein (GFP) transgenes, one expressed in the pharyngeal muscles (*myo-2::GFP*) and the other expressed in the body-wall muscles (*myo-3::GFP*). To initiate RNAi, a third transgene was introduced that expresses a GFP dsRNA construct under the control of the pharynx-specific *myo-2* promoter (*myo-2::GFP dsRNA*) (*15*). In HC57, localized RNAi of *myo-2::GFP* in the pharynx was highly penetrant, but incomplete and temperature sensitive (Fig. 1B, compare with 1A), whereas systemic RNAi of *myo-3::GFP* in body-wall muscle was position-dependent and also temperature-sensitive (Fig. 1, B and C) (*15*). Systemic RNAi did not require expression of GFP in the pharynx, as expression of only *myo-2::GFP dsRNA* led to silencing of GFP in body-wall muscle (Fig. 1D). Silencing in both the pharynx and body-wall muscles was dependent on *rde-1*, verifying that the silencing was due to RNAi (Fig. 1G).

We used the HC57 strain to identify systemic RNA interference defective (*sid*) mutants, by screening for animals resistant to systemic RNAi of *myo-3::GFP* in the body-

Department of Molecular and Cellular Biology, Harvard University, 16 Divinity Avenue, Cambridge, MA 02138, USA.

*To whom correspondence should be addressed. E-mail: hunter@mcb.harvard.edu

wall muscles, but still sensitive to cell-autonomous RNAi of *myo-2::GFP* in the pharynx (*15*). To enhance the sensitivity of the screen, we incorporated bacteria-mediated RNAi of GFP to completely eliminate expression of *myo-3::GFP* (Fig. 1F) (*15*). Prospective *sid* mutants expressed GFP strongly in body-wall muscles, but continued to show weak GFP expression in pharyngeal cells. We identified at least 106 independent *sid* mutants that define three major complementation groups [*sid-1, -2, -3* (48, 33, and 25 recessive alleles, respectively)]. Here, we describe the characterization and isolation of *sid-1*.

sid-1 mutants retain cell-autonomous RNAi in the pharynx, fail to show spreading of RNAi from the pharynx into the body-wall, and are completely resistant to bacteria-mediated RNAi of *myo-3::GFP* (Fig. 1H). *sid-1* exhibits no other obvious phenotype and produces an approximately normal-sized brood.

To further characterize systemic RNAi resistance in *sid-1* mutants, dsRNAs targeting different classes of mRNAs were introduced into a reference allele (*qt2*) by a variety of methods. To show that *sid-1(qt2)* is not simply deficient for RNAi in body-wall muscle cells, we introduced a transgene expressing GFP dsRNA in body-wall muscle cells. This transgene effectively silenced GFP expression in wild-type and *sid-1* muscle cells, consistent with *sid-1* specifically affecting systemic RNAi (*15*, *16*). As expected for a gene required for systemic RNAi, *sid-1(qt2)* worms show resistance to bacteria-mediated RNAi targeting both somatic (*unc-22*, *unc-54*) and germ line (*mex-3*, *mex-6*) expressed genes [Table 1 (*17*)].

Systemic RNAi can also be assayed by injecting dsRNA into either the intestine or the syncitial germ line within the gonad. Injection of a few cell volumes of *mex-3* dsRNA into the intestine of adult wild-type hermaphrodites effectively targets germ line *mex-3* transcripts, producing an embryonic lethal phenotype (Table 1A) (*15*). Injections into *sid-1*(*qt2*) hermaphrodites produced only viable progeny (Table 1A), demonstrating that the RNAi response cannot spread from the intestine to the germ line in *sid-1* mutants. When *mex-3* dsRNA was injected into *sid-1(qt2)* gonad arms, embryonic lethality was observed, showing that *sid-1* is not required for RNAi in the

Table 1. Characterization of *sid-1* systemic RNAi resistance. Progeny of *sid-1*(*qt2*) and wild-type (WT) worms exposed to *mex-3* and *unc-22* dsRNA by various methods were scored for RNAi phenotypes. Asterisks indicate that only cross progeny were scored. NA, not applicable; number of progeny scored, in parentheses.

dsRNA delivery (hours after injection) (A) *mex-3* RNAi	Percent embryonic lethal	
	Wild-type N2	*sid-1* (*qt2*)
Bacteria-mediated (NA)	100 (615)	1 (535)
Intestine (12.5 to 24.5)	86 (665)	2 (782)
(B) *unc-22* RNAi	Percent twitching progeny	
	Wild-type N2	*sid-1*(*qt2*)
Bacteria-mediated (NA)	100 (394)	0 (363)
Intestine (11 to 23)	68 (701)	0 (563)
Intestine crossed to WT males (7.5 to 31.5)	70 (497)*	14 (571)*
Anterior gonad arm (15.5 to 42.5)	89 (688)	0 (981)
Both gonad arms (7 to 40.5)	80 (886)	2 (1050)
Both gonad arms crossed to WT males (12 to 24)	99 (206)*	63 (380)*
	sid-1(*qt2*) *dpy-11*/++ (Dpy-11 progeny scored)	
Intestine (9.5 to 24.5)	96 (147)	
Both gonad arms (9.5 to 24.5)	98 (127)	

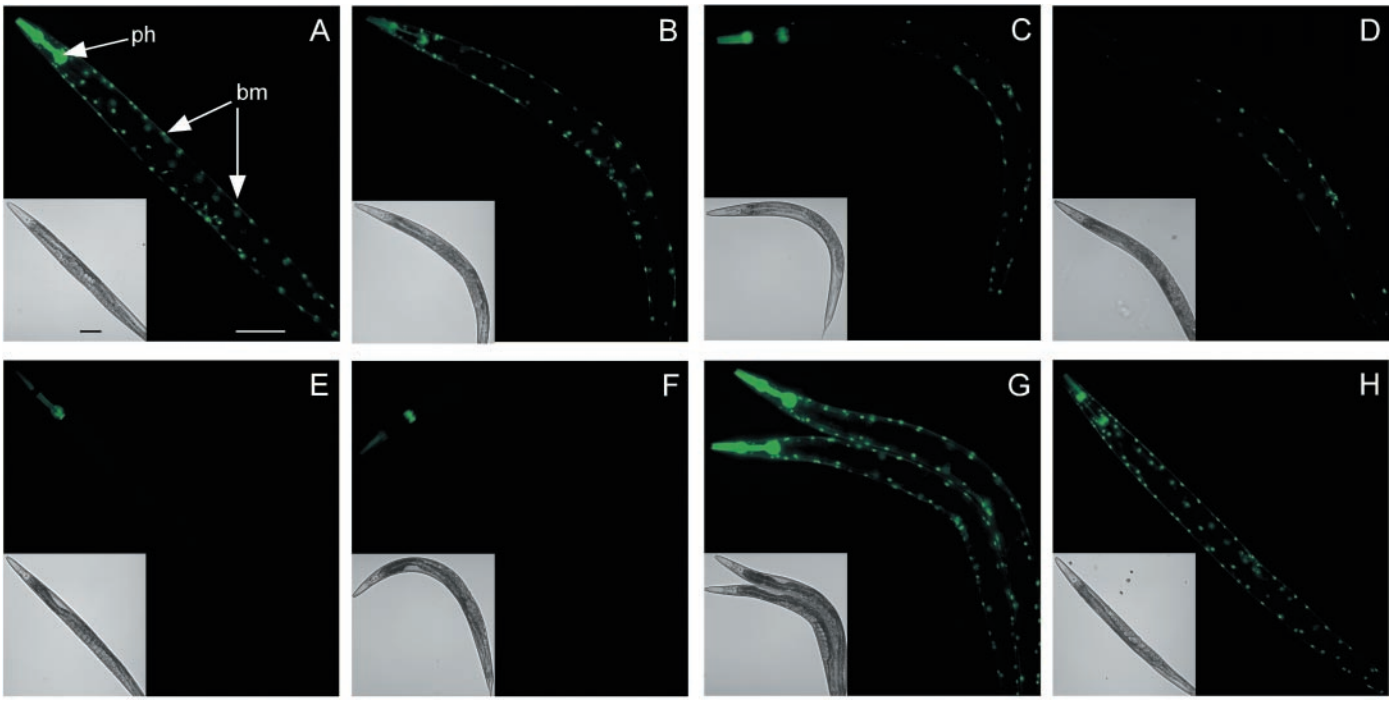

Fig. 1. Visualization of systemic RNAi. (**A**) HC46 strain expressing GFP in pharynx (ph) and body-wall muscle (bm) (25°C). (**B** and **C**) HC57 strain in which the pharynx-driven GFP dsRNA hairpin has been introduced into the HC46 background at 25°C (B) and 20°C (C). (**D**) HC59 strain expressing GFP dsRNA in the pharynx and GFP in only the body-wall muscles. (**E** and **F**) Bacteria-mediated RNAi of GFP in HC46 (E) and HC57 (F) at 20°C. (**G**) *rde-1*(*ne219*) in the HC57 background (20°C). (**H**) *sid-1*(*qt2*) in the HC57 background at 20°C. All images are of adult hermaphrodites taken at equal exposures. Insets are white-light images of the corresponding worm(s). Anterior is to the left. Scale bars, 0.1 mm.

germ line. In contrast to wild-type hermaphrodites, which when injected with *mex-3* dsRNA directly into either one or both gonad arms produced nearly 100% embryonic lethality, injection of *mex-3* dsRNA into just the anterior gonad arm of *sid-1(qt2)* worms only produced up to approximately 50% embryonic lethality in the progeny (Fig. 2A). These experiments show that *sid-1* is required to spread the RNAi effect to the germ line cells in the other gonad arm.

RNAi can also be transmitted to the progeny of injected animals (*1*). To determine whether this requires *sid-1* and therefore systemic RNAi, we analyzed silencing of *unc-22* in the progeny of injected worms. Injecting either the intestine or the gonad of wild-type hermaphrodites with *unc-22* dsRNA efficiently produces a twitching phenotype among their progeny (*1*, *15*). We found by similar injections that *sid-1* is required for transmission of RNAi to the progeny (Table 1B). We then asked whether supplying *sid-1*(+) to the embryos could restore systemic RNAi. We injected *unc-22* dsRNA into the gonad of *sid-1*(*qt2*) hermaphrodites and crossed them to wild-type males to determine whether the *sid-1*/+ progeny were now susceptible to *unc-22* RNAi. We found that the *sid-1*/+ progeny were susceptible (Table 1B). This suggests that embryos that inherit either dsRNA or an autonomous RNAi response require *sid-1* function to transmit the effect to somatic tissues, perhaps indicating that transmission of RNAi to the progeny requires systemic spread of an amplified RNAi signal (*18*, *19*).

The identity of *sid-1* was determined by genetic mapping and DNA transformation rescue and corresponds to the predicted open reading frame C04F5.1 [Web figs. 1 and 2 (*15*)]. To confirm the structure of the predicted gene and to verify the identity as *sid-1*, we isolated and sequenced wild-type complementary DNA (cDNA) and mutant genomic DNA (gDNA) (*15*). cDNA sequencing revealed an extra 387 bp (exon 4) not found in the reported genomic sequence of C04F5.1. Sequencing gDNA confirmed that 1014 nucleotides are missing from coordinate 5122952 of the curated genomic sequence. The exon/intron structure and predicted domains of the revised gene are shown in Fig. 2B. Sequencing gDNA from 10 mutant alleles confirmed that C04F5.1 corresponds to *sid-1* (Fig. 2B). SID-1 is predicted to encode a 776–amino acid protein with 11 transmembrane domains with nematode, human, and mouse homologs [Web fig. 3 (*15*)].

Because *sid-1* is required for systemic RNAi and is predicted to be transmembrane, it is reasonable to predict that it is required for the import or export of a systemic RNAi signal. To determine whether SID-1 is required autonomously to import a bacteria-mediated RNAi signal or whether it can function nonautonomously to deliver a signal from a neighboring cell, we analyzed *sid-1* genetic mosaics. A *sid-1(qt2)* strain expressing *myo-3::GFP* was injected with *sid-1* gDNA and *myo-3::DsRED2* to produce an extrachromosomal array that both rescues *sid-1*(*qt2*) and expresses the red fluorescent protein DsRED2 in body-wall muscle cells (*15*). Because extrachromosomal arrays are mitotically unstable, these lines produce mosaic worms composed of both DsRED2(+), *sid-1*(+) cells and DsRED2(–), *sid-1*(–) cells. If *sid-1* functions cell-autonomously, then

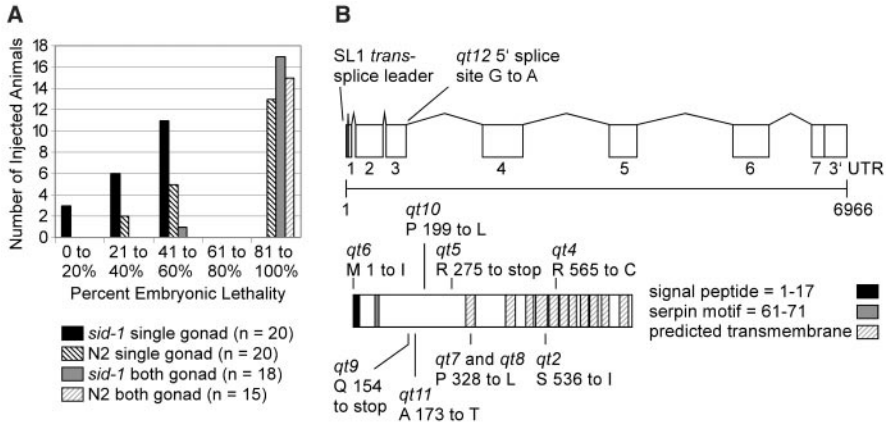

Fig. 2. Autonomy and dose dependence of RNAi in *sid-1* and wild-type gonads and *sid-1* predicted gene structure. (**A**) *sid-1* is required for systemic RNAi between gonad arms. Progeny of *sid-1*(*qt2*) and wild-type hermaphrodites injected with *mex-3* dsRNA (1 mg/ml) in one or both gonad arms were scored for viability. Injection of 100, 10, and 1 μg/ml *mex-3* dsRNA into both gonad arms showed similar effects at a given concentration (*17*). (**B**) Predicted *sid-1* gene structure, protein domains, and sequenced mutations. The *qt12* 5′ splice-site mutation following exon 3 is predicted to terminate translation seven amino acids after amino acid 142.

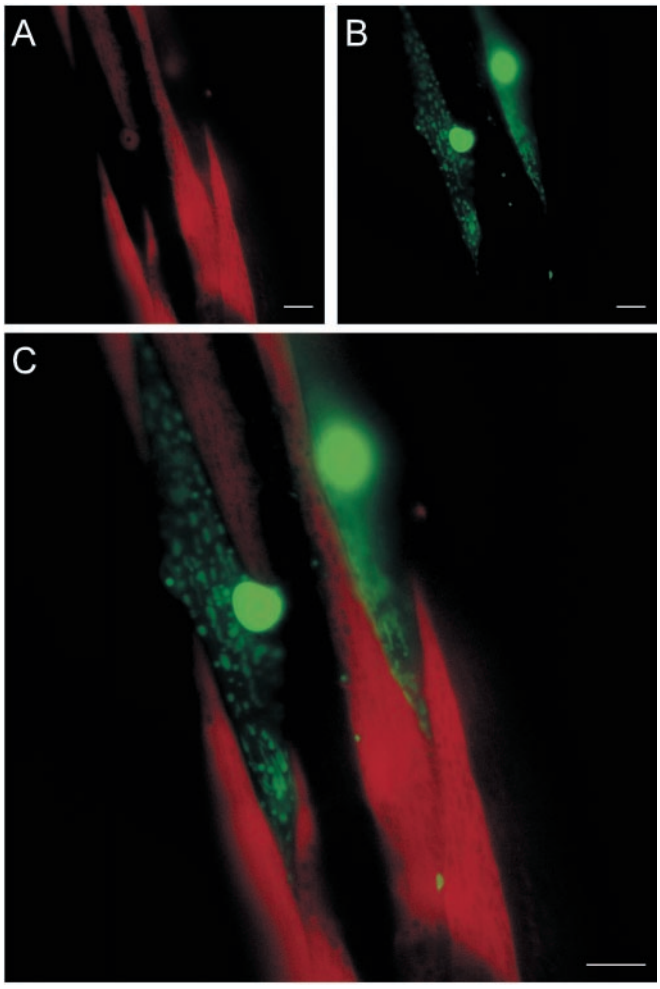

Fig. 3. Mosaic analysis of *sid-1* function. (**A**) *sid-1*(+) body-wall muscle cells are marked by the coexpression of DsRED2 (red). (**B**) Two muscle cells resistant to bacteria-mediated RNAi retain expression of GFP (green). (**C**) Only *sid-1*(+) muscle cells lose GFP expression. Scale bars, 10 μM.

DsRED2(+), *sid-1*(+) muscle cells will be sensitive to systemic RNAi of GFP, whereas DsRED2(–), *sid-1*(–) cells will be resistant. If *sid-1* functions nonautonomously, then DsRED2(–), *sid-1*(–) cells may be sensitive to systemic RNAi if they are adjacent to DsRED2(+), *sid-1*(+) cells. To distinguish between these possibilities, we exposed *sid-1* mosaic worms to bacteria expressing GFP dsRNA and examined DsRED2 expression at the boundaries between GFP-silenced muscle cells and those that were not silenced. In all 35 scored boundaries, cells that were sensitive to systemic RNAi (GFP silenced) were *sid-1*(+) (DsRED2 expressed), and cells that were resistant (GFP expressed) were *sid-1*(–) (DsRED2 not expressed) (Fig. 3). Although these results do not address the possibility that *sid-1* may function in the export of a systemic RNAi signal, they do show that *sid-1* is required to import or process one.

To determine when and where *sid-1* is expressed, we introduced transcriptional and translational *sid-1*::GFP transgenes into wild-type animals. A transgene that includes only the *sid-1* promoter region fused to GFP (*sid-1 pro::GFP*), is expressed in late embryos and continues to be detected in nearly all nonneuronal cell types through adulthood [Web fig. 4 (*15*)]. Interestingly, the highest levels of GFP expression in the adult are in the cells and tissues in direct contact with the environment. These environment-exposed cells also show expression of a transgene construct in which GFP was fused to the COOH-terminus of full-length SID-1 (*sid-1::C-GFP)* (Fig. 4) (*15*). This construct was capable of rescuing *sid-1*(*qt2*) animals, suggesting that localization of this reporter is representative of SID-1 localization. In addition to cytoplasmic expression, significant enrichment of subcellular localization of SID-1::C-GFP was seen at the cell periphery, consistent with the presence of predicted transmembrane regions in SID-1 (Fig. 4, K and L). Expression of SID-1::C-GFP was only seen in these environment exposed cells, perhaps because of the significantly lower expression of the translational reporter relative to the transcriptional reporter.

sid-1 functions cell-autonomously for systemic RNAi, encodes a protein with a signal peptide sequence and 11 putative transmembrane domains, and localizes a GFP protein fusion to the cell periphery. These observations suggest that *sid-1* may act as a channel for dsRNA, siRNAs, or some undiscovered RNAi signal. An additional possibility is that *sid-1* may be necessary for endocytosis of the systemic RNAi signal, perhaps functioning as a receptor. Consistent with the cell-autonomous requirement for *sid-1* function and the global nature of systemic RNAi, we detected *sid-1*::GFP in most nonneuronal cells. The failure to detect *sid-1*::GFP in the majority of neuronal cells is consistent with the observation that neuronal cells are generally resistant to systemic, but not autonomous RNAi (*20*). Notably, the few neurons that strongly express *sid-1* have externally exposed axons [phasmids and male rays (*17*)]. Similarly, the nonneuronal cells with the strongest *sid-1*::GFP levels are also the cells and tissues exposed to the environment. This suggests that *sid-1* may be involved in responding to environmental cues that may include viral and microbial pathogens. Finally, the absence of a detectable *sid-1* homolog in *Drosophila* is consistent with the apparent lack of systemic RNAi in *Drosophila* (*21*, *22*), whereas the strong similarity to predicted human and mouse proteins suggests the possibility that RNAi is systemic in mammals and that the mechanism may share some components found in *C. elegans*.

Note added in proof: Transmission of RNAi to progeny has recently been reported in *Tribolum* (Coleoptera) (*23*).

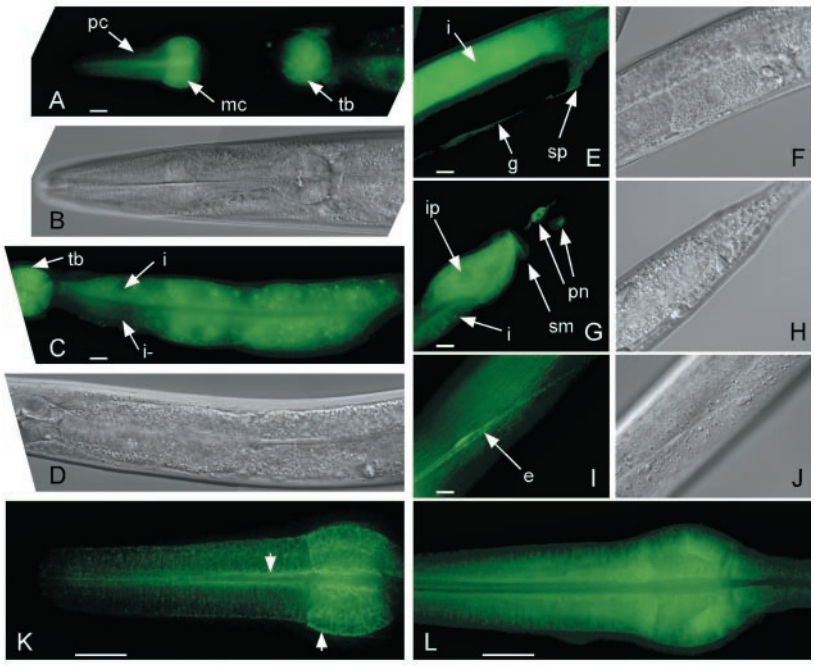

Fig. 4. SID-1::C-GFP reporter expression patterns. SID-1::C-GFP is expressed in (**A**) the procorpus (pc), metacorpus (mc), and terminal bulb (tb) of the pharynx; (**C**) intestine (i); (**E**) spermatheca (sp) and proximal somatic gonad (g); (**G**) sphincter muscles (sm), phasmid neurons (pn), and extreme posterior intestinal cells (ip), which is stronger compared to more anterior intestinal cells (i); and in (**I**) the excretory cell where it is localized throughout the tubular processes. Because the SID-1::C-GFP expression array is not integrated, mosaic expression patterns are observed. [In (C) a poorly expressing or not expressing intestinal cell is marked (i-).] (**K**) Cell periphery localization (arrow heads) of SID-1::C-GFP compared with (**L**) cytoplasmic GFP (*myo-2::GFP*) in deconvolved images representing 0.9 μM section of the pharynx. (**B**, **D**, **F**, **H**, and **J**) Accompanying DIC images. Scale bars, 10 μM.

References and Notes

1. A. Fire *et al.*, *Nature* **391**, 806 (1998).
2. H. Tabara, A. Grishok, C. C. Mello, *Science* **282**, 430 (1998).
3. I. Maeda, Y. Kohara, M. Yamamoto, A. Sugimoto, *Curr. Biol.* **11**, 171 (2001).
4. L. Timmons, A. Fire, *Nature* **395**, 854 (1998).
5. L. Timmons, D. L. Court, A. Fire, *Gene* **263**, 103 (2001).
6. J. C. Palauqui, T. Elmayan, J. M. Pollien, H. Vaucheret, *EMBO J.* **16**, 4738 (1997).
7. M. Fagard, H. Vaucheret, *Plant Mol. Biol.* **43**, 285 (2000).
8. R. Marathe, R. Anandalakshmi, T. H. Smith, G. J. Pruss, V. B. Vance, *Plant Mol. Biol.* **43**, 295 (2000).
9. O. Voinnet, C. Lederer, D. C. Baulcombe, *Cell* **103**, 157 (2000).
10. P. A. Sharp, *Genes Dev.* 15, 485 (2001).
11. S. M. Elbashir, W. Lendeckel, T. Tuschl, *Genes Dev.* **15**, 188 (2001).
12. N. J. Caplen, S. Parrish, F. Imani, A. Fire, R. A. Morgan, *Proc. Natl. Acad. Sci. U.S.A.* **98**, 9742 (2001).
13. H. Tabara *et al.*, *Cell* **99**, 123 (1999).
14. S. Parrish, A. Fire, *RNA* **7**, 1397 (2001).
15. Supplementary figures and details of experimental procedures are available on *Science* Online at www.sciencemag.org/cgi/content/full/1068836/DC1.
16. Of 34 F1 transformed *sid-1*(*qt2*) worms showing RNAi of *myo-3::GFP* that were recovered, 27 produced transformed, *myo-3::GFP* RNAi F2 offspring.
17. W. M. Winston, C. Molodowitch, C. P. Hunter, unpublished observations.
18. C. Lipardi, Q. Wei, B. M. Paterson, *Cell* **107**, 297 (2001).
19. T. Sijen *et al.*, *Cell* **107**, 465 (2001).
20. N. Tavernarakis, S. L. Wang, M. Dorovkov, A. Ryazanov, M. Driscoll, *Nature Genet.* **24**, 180 (2000).
21. E. Fortier, J. M. Belote, *Genesis* **26**, 240 (2000).
22. A. Piccin *et al.*, *Nucleic Acids Res.* **29**, e55 (2001).
23. G. Bucher, J. Scholten, M. Klingler, *Curr. Biol.* **12** (3), R85 (2002).

24. Some nematode strains used in this work were provided by the *Caenorhabditis* Genetics Center, which is funded by the NIH National Center for Research Resources. We acknowledge the Washington University Genome Sequence Center for the unpublished *C. briggsae* information. We thank S. Wicks for sharing snip-SNP information before publication, A. Fire for plasmids, S. Mou for technical help, and D. Mootz and A. Kay for critical reading of the manuscript. A Beckman Young Investigator award and a National Science Foundation award to C.P.H supported this work. The GenBank accession number for sid-1 cDNA nucleotide sequence is AF478687.

10 December 2001; accepted 25 January 2002
Published online 7 February 2002;
10.1126/science.1068836
Include this information when citing this paper.